

# Imaging the Earth's Interior: the Angular Distribution of Terrestrial Neutrinos

Brian D. Fields<sup>†1,2</sup> and Kathrin A. Hochmuth<sup>\*2</sup>

<sup>1</sup>*Center for Theoretical Astrophysics, Department of Astronomy, University of Illinois*

<sup>2</sup>*Department of Physics, University of Illinois*

## Abstract

Decays of radionuclides throughout the Earth's interior produce geothermal heat, but also are a source of antineutrinos; these geoneutrinos are now becoming observable in experiments such as KamLAND. Heretofore, the (angle-integrated) geoneutrino flux has been shown to provide a unique probe of geothermal heating due to decays, and an integral constraint on the distribution of radionuclides in the Earth. In this paper, we calculate the angular distribution of geoneutrinos, which opens a window on the *differential* radial distribution of terrestrial radionuclides. We develop the general formalism for the neutrino angular distribution. We also present the inverse transformation which recovers the terrestrial radioisotope distribution given a measurement of the neutrino angular distribution. Thus, geoneutrinos not only allow a means to image the Earth's interior, but offering a direct measure of the radioactive Earth, both (1) revealing the Earth's inner structure as probed by radionuclides, and (2) allowing for a complete determination of the radioactive heat generation as a function of radius. Turning to specific models, we emphasize the very useful approximation in which the Earth is modeled as a series of shells of uniform density. Using this multishell approximation, we present the geoneutrino angular distribution for the favored Earth model which has been used to calculate geoneutrino flux. In this model the neutrino generation is dominated by decays of potassium, uranium, and thorium in the Earth's mantle and crust; this leads to a very "peripheral" angular distribution, in which 2/3 of the neutrinos come from angles  $\theta \gtrsim 60^\circ$  away from the downward vertical. We note that a measurement of the neutrino intensity in peripheral directions leads to a strong lower limit to the central intensity. We also note that there is some controversy about the abundance of potassium in the Earth's core; different geophysical predictions lead to strongly varying, and hence distinguishable, central intensities ( $\theta \lesssim 30^\circ$  from the downward vertical). Other uncertainties in the models, and prospects for observation of the geoneutrino angular distribution, are briefly discussed. We conclude by urging the development and construction of antineutrino experiments with angular sensitivity.

---

<sup>†</sup> bdfields@uiuc.edu

<sup>\*</sup> hochmuth@uiuc.edu

## I. INTRODUCTION

The decays of radioactive species within the Earth generate an important component of geothermal heat. However, a quantitative accounting of the radioactive energy generation of the Earth requires a detailed knowledge of the abundance distribution of the key long-lived radioisotopes—uranium, thorium and potassium—inside the Earth. Because our knowledge of these abundance distributions is incomplete, the radiogenic heat output is consequently model-dependent and thus uncertain. A fundamental diagnostic is the “Urey ratio” which measures the ratio  $P_{\text{rad}}/P_{\text{lost}}$  of total radioactive heat production to the surface heat loss. Current estimates span the range [1], [2]

$$P_{\text{rad}}/P_{\text{lost}} \sim 0.5 - 0.6 \tag{1}$$

which seems to suggest that radiogenic heating is a dominant heat source, but not the only one. It is even possible that the Urey ratio is closer to 1, as the primordial heat from Earth’s formation should have radiated away a long time ago [3], and so the Earth’s heat should be fully radiogenic. This would imply that more radioactive material is hidden in the Earth. The strength of these qualitative conclusions thus hangs on the strength of the quantitative measurements of the radiogenic heat production and total heat loss.

A beautiful if challenging means of measuring the radiogenic heat production of the Earth follows from the realization that  $\beta$ -decays not only are a heat source but also produce (anti)-neutrinos. Decades ago, the prescient work of Eder [4] and later Krauss, Glashow, and Schramm [5] pointed out that the radioactive heat flux and the neutrino flux from the Earth are tightly linked. A measurement of the neutrino flux would constrain the radiogenic heat production, and thus offer a new and direct measure of the Urey ratio. Clearly, a precise measurement of the Urey ratio would provide important insight into the interior structure and dynamics of the Earth.

This vision of neutrino geophysics has enjoyed a major advance recently, with the first detection of geoneutrinos by the KamLAND Collaboration [6]. In fact, the detection of these geoneutrinos was only a side product of the KamLAND detector, as it is primarily designed to detect the flavor change of reactor antineutrinos produced by the Japanese nuclear power plants. The KamLAND Collaboration reported a total of 9 geoneutrino events, of which they estimate 4 are from  $^{238}\text{U}$  decay, and 5 are from  $^{232}\text{Th}$  decay [6]. Obviously these are early days, but we are encouraged that, even in the presence of a dominant anthropogenic background, KamLAND has demonstrated that geoneutrinos exist at observable levels.

Several groups have taken interest in these neutrinos and have in conjunction with geophysi-

cists and geologists worked on models for the distribution of radioactive elements in the Earth and predicted the (angle-integrated) geoneutrino flux at different detector sites [7–11]. The flux calculations have already become rather sophisticated, and are based on detailed geophysical models, in some cases even including the effects of the anisotropic radioisotope densities in the crust. These models confirm in detail that indeed the geoneutrino heat flux is proportional to radiogenic heat flux, but with the important caveat that the exact scaling between the two depends on the detailed abundance and density distributions within the Earth.<sup>1</sup> In this sense, the geoneutrino flux measurement is an *integral* measure of the radioisotope distribution.

In this paper we want to consider the angular distribution of the geoneutrino flux. We show that, once well-measured, the angular distribution can be inverted to recover the full density distribution of radionuclides—a tomography of the structure and radiogenic heat generation of the Earth. In addition, we come to the conclusion that with a future low-energy antineutrino detector with even crude angular resolution, it will be possible to distinguish between the different Earth Models and solve the problem as to how much radioactive material is contained in the Earth and where it is located. Thus, the angular distribution provides a *differential* measurement of the radioisotope distribution, and can reveal a wealth of new information about the structure and content of the Earth.

We first present the formal calculations in §II. After outlining the general formalism, we consider the useful approximation of a uniform density shell, from which a multiple-shell model of the Earth can be constructed. We then review (§III) models for the radioisotopic content of the Earth. Using these models we construct physically motivated illustrations of plausible geoneutrino angular distributions (§IV). We present several plots for different geological abundance predictions, finding in general that the high radioisotope content of the crust leads to a large “peripheral” geoneutrino signal. We investigate the possibility of  $^{40}\text{K}$  in the core, as recently suggested by several groups [12–14]; if core  $^{40}\text{K}$  is at the high end of these predictions, then the resulting neutrino signal could be quite large and should lead to a readily observable central intensity peak. Finally, we present conclusions §V, and discuss the exciting possibilities that will arise when we are able to use neutrinos to image the interior of the Earth.

Before we begin the formal development, a word of clarification seems in order. Note that for

---

<sup>1</sup> It is true that, at least in a spherically symmetric Earth, the surface heat flux is directly related, via Gauss’ law, to the total mass of radionuclides (c.f. eq. 24). However, a simple Gauss’ law argument fails in the case of neutrinos, because at each point they are emitted isotropically, not just radially, and as we will see, the “sideways” neutrinos make a large contribution to the total surface geoneutrino flux.

brevity, we will refer to the emitted particles as neutrinos, although they are of course antineutrinos. In fact, there is some regular  $\nu_e$  production due to  $^{40}\text{K}$  electron captures. However, the branching here is 10.72 % of all  $^{40}\text{K}$  decays, and thus the majority of the  $^{40}\text{K}$  nuclei  $\beta$ -decay and yield  $\bar{\nu}_e$  with a continuous energy spectrum. We look forward to the day when the monoenergetic  $^{40}\text{K}$  electron capture  $\nu_e$  flux (and angular distribution!) can be measured and compared against the  $\bar{\nu}_e$  signal. However, in this paper we will consider only the dominant,  $\beta$ -decay  $\bar{\nu}_e$  signals from K, Th, and U.

## II. FORMALISM

The fundamental quantity we wish to calculate is the differential intensity  $I$ , or surface brightness, of geoneutrinos at the surface of the Earth. This is just the distribution of neutrino flux  $F$  versus solid angle:  $I(\theta, \phi) = dF/d\Omega$ . Both angular coordinates are local and observer-centered:  $\theta \in [0, \pi/2]$  is the nadir angle, i.e., the angle measured from the downward vertical (so that the center of the Earth is at  $\theta = 0$ , and the horizontal is at  $\theta = \pi/2$ ; see Figure 1). The angle  $\phi$  is an azimuth. These angles thus cover the “sky” underfoot (or rather, the terrestrial hemisphere) which we wish to image. In this paper we will consider only the case of a spherically symmetric Earth (including the outermost layers). This guarantees that the intensity  $I = I(\theta)$  is azimuthally symmetric and so only depends on the nadir angle. In this case, we have  $I(\theta) = (2\pi)^{-1}dF/d\cos\theta$ .

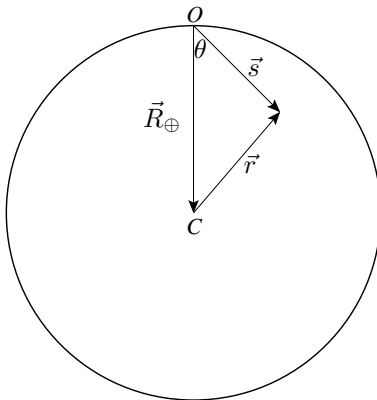


FIG. 1: The basic geometry of the problem. An observer at point  $O$  measures an intensity, which sums the emission along a line of sight  $\vec{s}$ . The nadir  $\vec{R}_\oplus$  points to the center  $C$  of the Earth, which makes an angle  $\theta$  with the line of sight. A given point along  $\vec{s}$  is at geocentric distance  $\vec{r}$ .

The neutrino intensity in any direction depends on the distribution of sources along that line of sight. The governing equation is that of radiation transfer for neutrinos, which is formally identical to the usual expression for photons [15], although of course the microphysics is quite different (the

Earth is optically thin to neutrinos, but neutrinos do undergo oscillations). Then over a line of sight  $\vec{s}$ , ignoring scattering and absorption, the intensity changes according to

$$dI/ds = q(\vec{s})/4\pi \quad (2)$$

where  $q$  is the source function at point  $\vec{s}$ , which measures the local neutrino production rate per unit volume.

For each radioisotope species  $i$ , this takes the form

$$q_i = \frac{n_i}{\tau_i} = \frac{\rho_i}{\tau_i m_i} \quad (3)$$

Here  $n_i$  and  $\rho_i$  are the local number and mass densities, respectively, of species  $i$  in the Earth. The  $\tau_i$  is the mean lifetime and  $m_i$  is the mass of an  $i$  nucleus. The total source is just a superposition of all species:  $q = \sum_i q_i$ . The effects of neutrino oscillations are not yet included; we will address this below (§II B).

Integrating eq. (2) over a line of sight at nadir angle  $\theta$ , we find the intensity

$$I(\theta) = \int_0^{2R_\oplus \cos \theta} q(\vec{s}) ds \quad (4)$$

where  $\vec{s}$  is centered on the observer, as seen in Figure 1.

Since models of the Earth's structure and composition are expressed in terms of the radius  $\vec{r}$ , it is very useful to rewrite eq. (4) in these geocentric coordinates. From Figure 1 we see that the  $\vec{s} = \vec{r} + \vec{R}_\oplus$ , so that  $\vec{r} = \vec{s} - \vec{R}_\oplus$  and thus

$$s(r, \theta) = R_\oplus \cos \theta \pm \sqrt{r^2 - (1 - \cos^2 \theta) R_\oplus^2} \quad (5)$$

where  $\pm$  corresponds to the far side (near side) of the midpoint  $s = R_\oplus \cos \theta$  of the line of sight. Therefore, for a fixed nadir angle  $\theta$ , we can transform the integral to the geocentric coordinate system:

$$I_i(\theta) = 2 \int_{R_\oplus \sin \theta}^{R_\oplus} dr \frac{q_i(r) r}{\sqrt{r^2 - (1 - \cos^2 \theta) R_\oplus^2}} \quad (6)$$

where  $q_i(r)$  can in a non-spherically symmetric case also be a function of (geocentric) latitude and longitude. In this case, the factor of 2 is replaced by the sum of integrals for the near-side and the far-side of the midpoint  $s = R \cos \theta$ . In our special case of spherical symmetry, the contribution from the near half of the sphere is the same as the contribution from the far side.

Equation (6) explicitly demonstrates that the intensity  $I(\theta)$  is an integral transformation of the source distribution  $q(r)$ . In fact, this mapping is a form of the Abel transform [16], which is

used in deprojection problems in both astrophysics [17] and geophysics [18]. Thus it is clear that a determination of the intensity distribution offers a measure of the source distribution. Namely, one can invert the transformation (deproject the image) to fully recover the complete source distribution  $q(r)$ ; this inversion procedure is explicitly presented in Appendix A. In other words, *a measurement of the angular distribution of geoneutrinos not only yields an image of the Earth's radioactive interior, but this image can also be inverted to give a tomography of the terrestrial radioisotope distribution.* Clearly, the geoneutrino angular distribution offers a unique and powerful probe of the interior of the Earth. This power will be further illustrated below, where we will see that even a partial (low-resolution) determination of  $I(\theta)$  offers important geophysical information.

In evaluating eq. (6), it will be convenient to introduce dimensionless scaled variables: a radial fraction  $x = r/R_\oplus \in [0, 1]$ , a local mass fraction  $a_i = \rho_i/\rho$ , and a local density measure  $\tilde{\rho} = \rho/\bar{\rho}$  (with  $\bar{\rho} = 3M/4\pi R_\oplus^3$  the mean Earth density). It will also be useful to denote the nadir angle cosine as  $\mu = \cos \theta$ . We then rewrite eq. (6) as a product of two terms

$$I_i(\theta) = I_{i,0} g_i(\mu) \quad (7)$$

Here the dimensionful overall magnitude is set by

$$I_{i,0} = 2 \frac{N_i \bar{a}_i \bar{\rho} R_\oplus}{4\pi A_i \tau_i m_u} \quad (8)$$

where  $N_i$  is neutrino multiplicity, i.e., the number of geoneutrinos released per decay chain. Values of  $I_{i,0}$  appear in Table I. The dimensionless angular distribution or (akin to the ‘‘phase function’’ of radiation transfer [15]) is the heart of this paper, and is contained in the function

$$g_i(\mu) = \int_{\sqrt{1-\mu^2}}^1 dx \frac{\tilde{\rho}_i(x) x}{\sqrt{x^2 - (1 - \mu^2)}} \quad (9)$$

which requires knowledge of the density distribution of each radioisotope, usually presented in terms of mass fractions  $a_i$  and a total density profile  $\rho$  via  $\tilde{\rho}_i = \rho_i/\bar{\rho}_i = (a_i/\bar{a}_i)\tilde{\rho}$ .

The flux of geoneutrinos integrated over different annuli is also of interest. We quantify this in terms of the flux *exterior* to the nadir angle  $\theta$ , via

$$F_i(> \theta) = F_i(< \mu) = \int_{\Omega_{\text{shell}}} d\Omega I_i(\mu, \phi) \quad (10)$$

$$= 2\pi I_{i,0} \int_0^\mu d\mu g(\mu) \quad (11)$$

$$\equiv 2\pi I_{i,0} H(\mu) \quad (12)$$

where second and third expressions assume spherical symmetry, and where the dimensionless quantity  $H$  encodes the angular dependence. A consequence of this definition is that the total neutrino

flux is given by  $F_i(\theta > 0) = F_i(\mu < 1) = 2\pi I_{i,0} H(1)$ . This can be compared with existing calculations [5, 8, 10].

TABLE I: Properties of the Principle Geoneutrino Source Nuclei

Radioisotope	mean life	$\bar{\nu}_e$ multiplicity	isotopic	mean terrestrial	intensity normalization
species	$\tau$ (Gyr)	$N_i$	abundance	abundance $\bar{a}_i$	$I_{i,0}$ [neutrinos $\text{cm}^{-2} \text{s}^{-1} \text{sr}^{-1}$ ]
$^{40}\text{K}$	1.84	1	0.0117%	$1.8 \times 10^{-8}$	$2.4 \times 10^6$
$^{238}\text{U}$	6.45	6	99.2745%	$5.3 \times 10^{-8}$	$0.48 \times 10^6$
$^{232}\text{Th}$	20.3	4	100%	$1.35 \times 10^{-8}$	$0.56 \times 10^6$

### A. The Uniform Shell Approximation

We want to consider a single shell with a density  $\tilde{\rho}_{i,0}$  in species  $i$  which is constant between  $r_{\text{in}} = x_{\text{in}} R_{\oplus}$  and  $r_{\text{out}} = x_{\text{out}} R_{\oplus}$ , and zero otherwise:

$$\tilde{\rho}_i(x) = \begin{cases} \tilde{\rho}_{i,0} & x_{\text{in}} < x < x_{\text{out}} , \\ 0 & \text{otherwise} \end{cases} \quad (13)$$

This form allows us to simplify the integral and solve it analytically. In particular, owing to the constant density, the intensity at each line of sight is just proportional to the shell path length  $\Delta s(\theta)$  along that sightline.

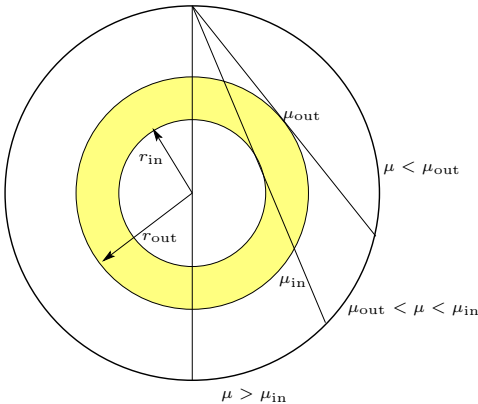


FIG. 2: Geometry for the uniform shell model. The inner and outer shell radii are  $r_{\text{in}}$  and  $r_{\text{out}}$ , respectively. The lines of sight tangent to the inner and outer edges of the shell are shown, and are at nadir angle cosines  $\mu_{\text{in}}$  and  $\mu_{\text{out}}$ , respectively. These lines of sight divide the terrestrial hemisphere into three distinct regions, which are labeled.

There are three cases to be distinguished, as one can see in Figure 2:

$$g(\mu) = \begin{cases} \tilde{\rho}_{i,0} \left( \sqrt{\mu^2 - \mu_{\text{out}}^2} - \sqrt{\mu^2 - \mu_{\text{in}}^2} \right) , & \mu > \mu_{\text{in}} \\ \tilde{\rho}_{i,0} \sqrt{\mu^2 - \mu_{\text{out}}^2} , & \mu_{\text{out}} \leq \mu \leq \mu_{\text{in}} \\ 0 , & \mu < \mu_{\text{out}} \end{cases} \quad (14)$$

where

$$\mu_{\text{in}} = \sqrt{1 - x_{\text{in}}^2} , \quad \mu_{\text{out}} = \sqrt{1 - x_{\text{out}}^2} . \quad (15)$$

These are integrable, and give

$$H(\mu) = \begin{cases} \frac{\tilde{\rho}_{i,0}}{2} [\mu_{\text{out}}^2 h(\mu/\mu_{\text{out}}) - \mu_{\text{in}}^2 h(\mu/\mu_{\text{in}})] , & \mu > \mu_{\text{in}} \\ \frac{\tilde{\rho}_{i,0}}{2} \mu_{\text{out}}^2 h(\mu/\mu_{\text{out}}) , & \mu_{\text{out}} \leq \mu \leq \mu_{\text{in}} \\ 0 & \mu < \mu_{\text{out}} \end{cases} \quad (16)$$

where

$$h(u) = \frac{1}{2} u \sqrt{u^2 - 1} - \frac{1}{2} \ln \left( u + \sqrt{u^2 - 1} \right) . \quad (17)$$

Note that eq. (16) calls  $h(u)$  only in the domain  $u \geq 1$ , and that  $h(1) = 0$ . The total flux for a uniform shell was first calculated in [5], and one can easily show that  $F(\mu < 1)$  reproduces their result.

There are four cases we want to illustrate; these are plotted in Figure 3. In the “uniform Earth” model, the density is the same throughout the whole planet ( $x_{\text{in}} = 0$ ,  $x_{\text{out}} = 1$ ). This gives an angular distribution which grows linearly with  $\mu$ ,  $g(\mu) = \tilde{\rho}_{i,0}\mu$ , and hence  $I(\theta) \propto \cos(\theta)$ . The integrated flux which increases quadratically as  $H(\mu) = \tilde{\rho}_{i,0}\mu^2/2$ , i.e.,  $H(\theta) \propto \cos^2\theta$ . This therefore gives a very centrally bright distribution. In the “uniform core” model, the density is non-zero only in a central region which extends from  $x_{\text{in}} = 0$  to  $x_{\text{out}}$ . As seen in Figure 3, this gives an inner intensity distribution which is similar to the uniform Earth model, as one would expect, but which goes to zero, as it should, at the outer tangent  $\mu_{\text{out}}$ .

As we will see below, it turns out that a more physically motivated case is the “uniform crust” model, where only the layers of the Earth (from  $x_{\text{in}}$  to  $x_{\text{out}} = 1$ ) contribute. This yields an intensity distribution

$$g(\mu) = \begin{cases} \tilde{\rho}_{i,0} \left[ \mu - \sqrt{\mu^2 - \mu_{\text{in}}^2} \right] , & \mu > \mu_{\text{in}} \\ \tilde{\rho}_{i,0}\mu , & \mu \leq \mu_{\text{in}} \end{cases} \quad (18)$$

$$H(\mu) = \begin{cases} \frac{\tilde{\rho}_{i,0}}{2} [\mu_{\text{out}}^2 h(\mu/\mu_{\text{out}}) - \mu_{\text{in}}^2 h(\mu/\mu_{\text{in}})] , & \mu > \mu_{\text{in}} \\ \frac{\tilde{\rho}_{i,0}}{2} \mu^2 , & \mu \leq \mu_{\text{in}} \end{cases} \quad (19)$$



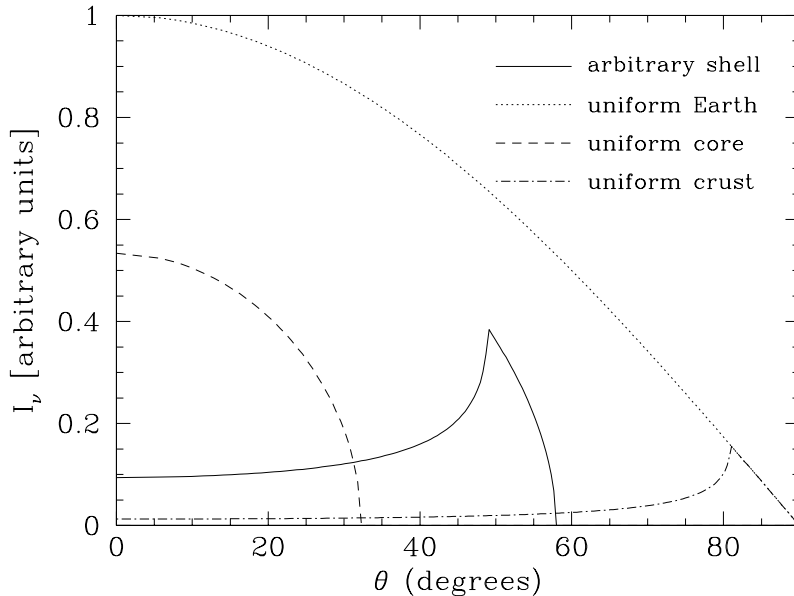


FIG. 3: The angular distribution of intensity for different cases of a 1-zone, uniform density model, shown as a function of nadir angle  $\theta$ . The units in the vertical scale are arbitrary, and the normalizations of the different curves are chosen for clarity.

which is also linear in  $\mu$ , and thus scales as  $I \propto \cos(\theta)$ , for large angles. The intensity peaks at inner tangent point  $\mu_{\text{in}}$ , where the line of sight is longest. A measurement of this peak would thus give the position of the inner edge. Interior to  $\mu_{\text{in}}$ , the intensity drops to a minimum at the nadir, where the column density is the smallest. But the central intensity is nonzero, and is simply related to the peak intensity via

$$\frac{I_{\text{peak}}}{I_{\text{center}}} = \frac{I(\mu_{\text{in}})}{I(1)} = \frac{\Delta s(\mu_{\text{in}})}{\Delta r_{\text{shell}}} = \sqrt{\frac{1+x_{\text{in}}}{1-x_{\text{in}}}} \quad (20)$$

This useful relation allows one to use the peripheral flux, due to emission from Earth's outer layers, to put a lower limit on the contribution of these layers to the central flux. Any observed central flux in excess of this limit must be due to emission from the inner Earth.

The last model illustrated in Figure 3 is a single shell with arbitrary inner and outer radii. The intensity distribution is an amalgam of the features seen in the special cases of the crust and core models. As with the crust model, the intensity peaks at the inner tangent point, where the line of sight is longest. As with the core model, the intensity goes to zero at the outer tangent. Thus, a measurements of the peak would give the position of the shell's inner edge, while a measurement of the cutoff would give the outer edge.

## B. Towards a Realistic multishell Model

Based on the idealized calculations in the last section we want to build now a model that is applicable for the Earth's Interior. The Earth of course does not have a constant density. However, we can approximate the density structure as a series of uniform density shells. Indeed, Earth models are in practice typically expressed in this manner. Formally, the generalization is trivial, thanks to the lack of neutrino absorption and scattering, which guarantees that superposition holds:

$$I_i(\theta) = \sum_{\text{shells } j} I_i^{(j)}(\theta) \quad (21)$$

$$F_i(> \theta) = \sum_{\text{shells } j} F_i^{(j)}(> \theta) \quad (22)$$

where  $I_i^{(j)}(\theta)$  and  $F_i^{(j)}(\theta)$  are the intensity and flux, respectively, from shell  $j$ .

Moreover we must consider the effect of neutrino oscillations [9, 11]. As the mass eigenstates of the neutrinos differ from the flavor eigenstates, some of the initial  $\bar{\nu}_e$  signal will be converted into other flavors during propagation, and thus reduce the  $\bar{\nu}_e$  signal in the detector. In general, the oscillations will have a ‘‘vacuum’’ contribution, but will be modified due to the MSW effect, which is density- and energy-dependent. If the MSW effect is important, then it complicates the determination of the angular distribution, introducing a density- and path-dependent MSW suppression factor into eq. (6) and its descendants. This factor would complicate the inversion of the angular distribution  $I(\theta)$  to recover the radioisotope source distribution  $q(r)$ .

However, geoneutrinos have a very low energy and as the Earth's density is much lower compared to stellar objects we do not expect, that the MSW effect plays any greater role. This can be justified if the vacuum oscillation length  $L_v$  is much smaller than the oscillation length in matter  $L_m$ . If we take the values of ref. [19] for the matter in the Earth and a value for  $\Delta m^2 \sim 10^{-4} \text{ eV}^2$ , we obtain  $L_v \sim 10 \text{ km}$  and  $L_m \sim 1000 \text{ km}$ . Therefore  $|L_v| \ll |L_m|$ , and we see that, roughly speaking, the vacuum oscillation length is short compared to both the the matter oscillation length and to the changes in density; thus the vacuum oscillations will wash out any matter effect and average out the pathlength dependence. We thus follow Mantovani et al. [10] and introduce only a density-independent oscillation probability of  $(1 - \frac{1}{2} \sin^2 2\vartheta_{12}) = 0.59$  in our equations. Here  $\vartheta_{12}$  is the electron-neutrino  $\nu_e - \nu_x$  mixing angle; solar neutrino experiments and KamLAND are best fit [20] by  $\sin^2 \vartheta_{12} = 0.315 \pm 0.035$  (and hence  $\sin^2 2\vartheta_{12} = 0.81$ ). and  $\Delta m^2 = (7.3 \pm 0.8) \times 10^{-5} \text{ eV}^2$ . Therefore the intensity scaling of eq. (8) changes to:

$$I_{i,0}^{\text{eff}} = \left(1 - \frac{1}{2} \sin^2 2\vartheta_{12}\right) I_{i,0} \quad . \quad (23)$$

Table I sums up the important properties of the radioactive elements in question.

In the next section we want to use this and discuss different Earth Models.

### III. EARTH MODELS

The geoneutrino intensity depends on the radioisotope density structure  $\rho_i(r)$ , which is usually presented as abundances  $a_i$  and a total density  $\rho$ , where  $\rho_i = a_i\rho$ . The Earth’s interior structure and total density are primarily probed via the propagation of seismic waves. These results have been synthesized by Dziewonski and Anderson in their Preliminary Reference Earth Model [21]. Following [10] we will adopt this model. In addition, for our spherically symmetric study we took the last three kilometers of the Earth to be sediments.

The distribution of radioisotope abundances  $a_i$  are obtained with different geological measurements which, for most of the Earth’s interior, are necessarily indirect. Consequently, the abundance distribution remains model-dependent. Indeed, the measurement of the angular distribution of geoneutrinos (as well as the geoneutrino energy spectrum) would provide a powerful new method to *measure* the radioisotope distribution. For the purposes of illustration here, we will adopt the values of  $a_i$  given in the reference model of Mantovani et al. [10], which are very detailed and draw on a wealth of geophysical data. This model takes into account the bulk silicate Earth model, which describes the composition of the crust-mantle system. Table II shows the adopted abundance distribution. Note that these are *elemental* abundances; we assume that the isotopic fractions of Table I hold throughout the Earth. This correction is particularly important for  $^{40}\text{K}$ .

TABLE II: Mantle and crust elemental abundance distribution [10].

Region	radii [km]	$a(\text{U})$	$a(\text{Th})$	$a(\text{K})$
Lower Mantle	3480–5600	$13.2 \times 10^{-9}$	$52 \times 10^{-9}$	$1.6 \times 10^{-4}$
Upper Mantle	5600–6291	$6.5 \times 10^{-9}$	$17.3 \times 10^{-9}$	$0.78 \times 10^{-4}$
Oceanic Crust	6291–6368	$0.1 \times 10^{-6}$	$0.22 \times 10^{-6}$	$0.125 \times 10^{-2}$
Lower Crust	6291–6346.6	$0.62 \times 10^{-6}$	$3.7 \times 10^{-6}$	$0.72 \times 10^{-2}$
Middle Crust	6346.6–6356	$1.6 \times 10^{-6}$	$6.1 \times 10^{-6}$	$1.67 \times 10^{-2}$
Upper Crust	6356–6381	$2.5 \times 10^{-6}$	$9.8 \times 10^{-6}$	$2.57 \times 10^{-2}$
Sediments	6368–6371	$1.68 \times 10^{-6}$	$6.9 \times 10^{-6}$	$1.7 \times 10^{-2}$
Oceans	6368–6371	$3.2 \times 10^{-9}$	0	$4.0 \times 10^{-4}$

The composition of the Earth’s core deserves special attention. The Earth’s core consists largely of iron. But its density is lower than one would expect if the core were pure iron. Therefore it is

assumed that light elements in the form of alloys are present [22]. So far it was generally believed, that the core does not hold any significant amount of radioactive elements, as there was no evidence that the radioactive isotopes in question could form alloys with iron. Hence, the Mantovani et al. [10] reference model places radioactive elements only in the mantle and in the crust, and are absent from the core.

On the other hand it is puzzling why solar chondrites have a K/U ratio that is eight times higher than in the crust-mantle system [23]. In this connection, it is noteworthy that recent experiments demonstrate that potassium does form alloys with iron under high temperature and pressure conditions which likely were present at Earth’s formation. The maximum possible amounts of potassium in Earth’s core suggested by the experiments range from 60-130 ppm [12], to 1200 ppm [14], to as high as 7000 ppm [13]. In light of these experiments, we will consider the possibility of an additional radiogenic contribution from the core, and quantify the impact of core  $^{40}\text{K}$  on the reference model.

The amount of radioactive material in the core contributes also to the radiogenic heat of the Earth. Presently the Earth’s surface loses about 40 TW or 87 mW/m<sup>2</sup>. The amount of surface radiation depends on convection and conduction properties of the Earth’s interior. The present day heat production  $H$  in units of TW of uranium, thorium and potassium with a total mass in kg of  $M_{\text{U}}$ ,  $M_{\text{Th}}$ ,  $M_{\text{K}}$  respectively is

$$H = \sum_i \epsilon_i M_i \approx 10 \left( \frac{M_{\text{U}}}{10^{17} \text{ kg}} \right) + 2.7 \left( \frac{M_{\text{Th}}}{10^{17} \text{ kg}} \right) + 3.4 \times 10^{-4} \left( \frac{M_{\text{K}}}{10^{17} \text{ kg}} \right) \text{ TW} \quad (24)$$

where  $\epsilon_i = Q_i/m_i\tau_{\beta,i}$  is the specific non-neutrino energy loss per nucleus, and where  $M_{\text{K}}$  is the *total* potassium mass, for which the  $^{40}\text{K}$  isotopic fraction appears in Table I. To obtain the heat production of potassium we used, that in 89.28% of all cases a  $^{40}\text{K}$  nucleus  $\beta$ -decays with a average energy of 0.598 MeV [24]. The other decay mode of potassium is electron capture with an energy of 1.505 MeV.

With knowledge of the radioisotopic content of the Earth from geoneutrinos, eq. (24) can be compared with the global heat flux, and used to determine the Urey ratio (eq. 1). While the radioisotope abundances remain uncertain, one can rather turn the problem around, and use the global heat flux with eq. (24) to set an upper limit to the radioisotopic content and thus to the geoneutrino flux. Such an analysis has been carried out by Mantovani et al., who find that this “maximal radiogenic” model leads to fluxes about twice the level of their reference model.

In the next section we will discuss the plots we created for the different Earth models.

## IV. RESULTS

We now combine our general formalism with various Earth models to arrive at predictions for the geoneutrino angular distribution. We first consider the reference model, then its variants and its uncertainties, and finally we comment on the effect of anisotropies in the radioisotope distributions.

### A. The Reference Model

The reference model of Mantovani et al. [10] serves as our standard and fiducial case. The geoneutrino intensity distribution for this model appears in Figure 4. We see that the total intensity is peaked near the horizon, at large nadir angles. The strikingly “peripheral” character of this neutrino distribution is a direct consequence of the location of the radioisotopes in the mantle and crust.

The experimental ability to detect this pattern is perhaps best quantified in Figure 5, which displays the cumulative angle-integrated flux  $F$  for the reference model (c.f. eq. 10). The change in the normalized flux  $F/F_{\text{tot}}$  over any angle interval gives the contribution of that interval to the total flux. Figure 5 thus shows that fully 2/3 of the total flux arrives in the outermost nadir angles  $\theta \gtrsim 60^\circ$ .

This model can thus be easily tested with an experiment having even the poorest angular resolution. For example, an experiment with  $30^\circ$  resolution could test whether the counts in the outer  $\theta > 60^\circ$  are a factor  $\sim 2$  higher than the counts in the inner  $\theta < 60^\circ$ . The confirmation of this model would vindicate the idea that U, Th, and K are indeed lithophilic elements that congregate in the mantle and crust.

Figure 4 also shows the expected angular distribution separately for uranium, thorium, potassium and the cumulative intensity for the reference model. The uranium to thorium ratio stays approximately the same, whereas the amount of potassium increases steeply in the crust. The intensity shows a double peak, which is due to the fact, that the abundance of radioactive elements is lower in the middle crust than in the upper and lower crust.

We note that the reference model gives a geoneutrino distribution qualitatively similar to the uniform crust model presented in §II. This of course traces to the positioning of the radioisotopes in the outer Earth. Of course the true geoneutrino behavior is more complicated, but it does appear that for a crude analysis (or in the presence of crude data) the uniform crust model would be a useful analytic approximation.

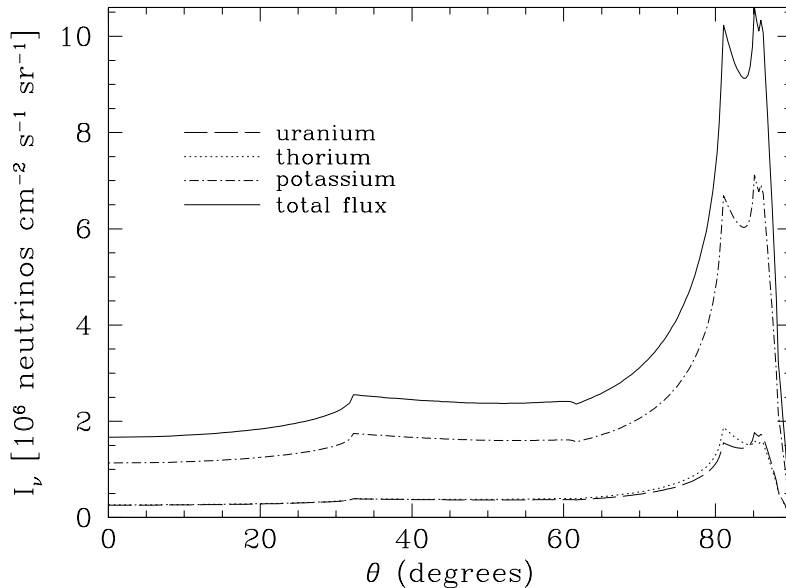


FIG. 4: The figure shows the reference model of ref. [10]. The dashed-dotted line represents the total expected intensity. No contribution coming from the core has been added yet. The other curves show the intensities from thorium, uranium and potassium separately. It can be seen that the major contribution is coming from potassium.

Finally, we wish to comment on the effects of sediments. We find that if the amount of sediments is increased by a factor of 10 the overall shape of the spectrum does not change except for a sharp peak towards  $90^\circ$ . An increase by a factor of two only increases the second peak slightly. Therefore we conclude, that the location of the detector will not change its ability to detect the structure of the mantle and crust.

### B. Models with Core Potassium

We now turn to the possibility that the Earth's core might contain significant amounts of  $^{40}\text{K}$ . Based on the experimental evidence that potassium can form alloys with iron we use the fiducial values obtained by different authors and add them to the reference model. We are aware that if the abundance ratios and mass ratios of the reference models are correct and only the total mass estimates of U, Th and K are incorrect, then the intensity of the neutrinos coming from the crust-mantle system should go down, but the overall shape should stay the same. This decrease in the peripheral intensity will make the core contribution even more dominant. On the other hand, it

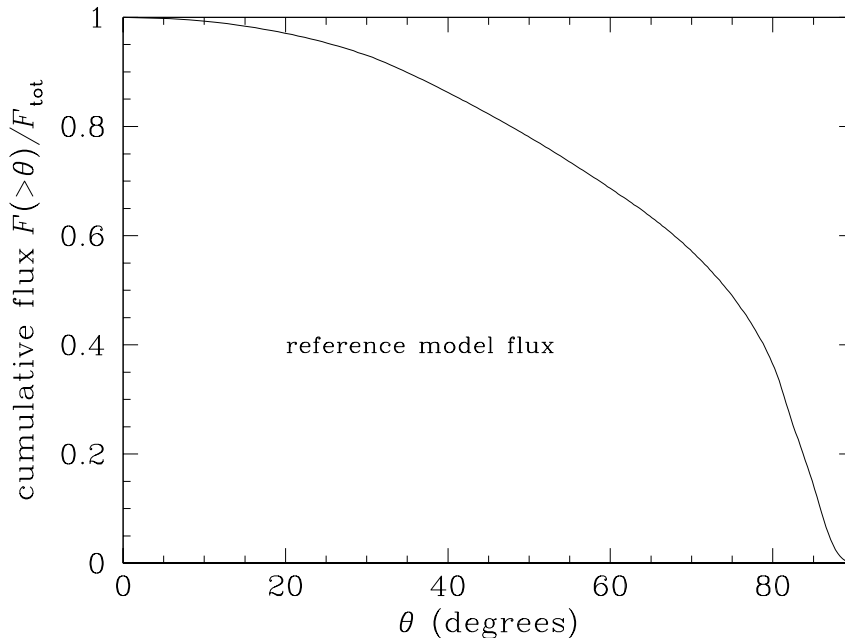


FIG. 5: Cumulative flux expected for the reference model. The flux is normalized to the total, and thus is dimensionless, spanning the range 0 to 1.

is possible that the assumptions of the reference model are correct (incorporating the bulk silicate Earth model with a heat production of  $\sim 20$  TW), but the Urey ratio is closer to 1 with a large amount of potassium in the core. In this case it is legitimate to add the core contribution to the reference model. In case of a fully radiogenic model with 20 TW coming from the crust-mantle system one would expect a total of  $\sim 330$  ppm of potassium in the core. Figure 6 shows the angular distribution for different amounts of potassium in the core as could be found in the literature, while Figure 7 shows the cumulative flux for the same models.

From Figures 6 and 7 it is clear that the introduction of  $^{40}\text{K}$  in the core can significantly alter the geoneutrino angular distribution. The effect is to enhance the central intensity ( $\theta \lesssim 30^\circ$ ), possibly also raising the overall detected flux. The departure from the reference model depends of course on the core potassium abundance. The value given in [13] of 7000 ppm potassium in the core is only an upper limit, but in this case the core would clearly dominate the distribution. For 1200 ppm of potassium in the core [14] the maximum intensities coming from crust and core are approximately the same. But even the much lower value obtained in [12] of 60-130 ppm might still be detectable with a future neutrino detector.

A future low energy neutrino detector with angular resolution will be able to distinguish be-

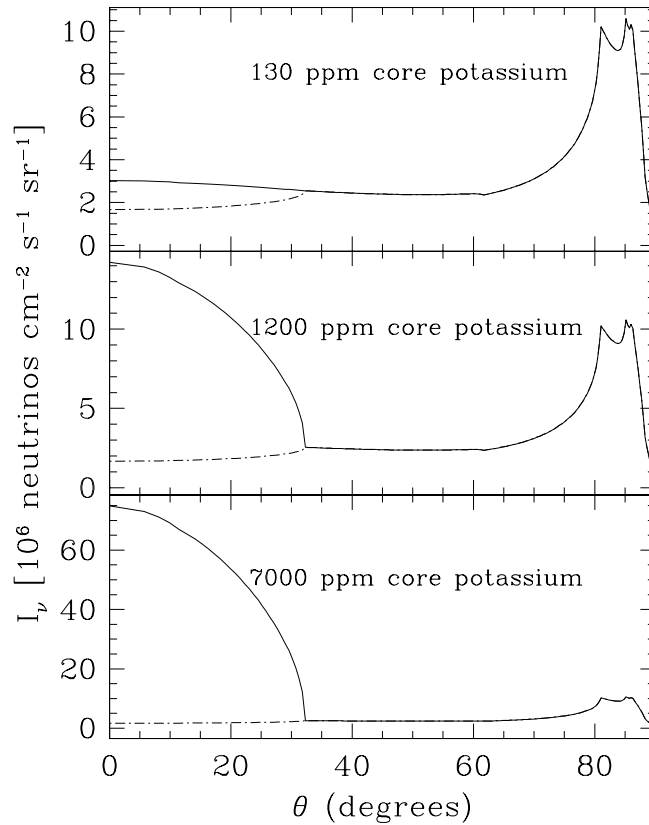


FIG. 6: The curves show the possible abundances for potassium in the core as found in [12], [13], [14]. The dashed-dotted line is the intensity of the reference model.

tween the opposing models. Again, with only a modest resolution, it will already be possible to make important statements. An experiment with  $30^\circ$  resolution could divide the emission into central, medial, and peripheral bins, and the relative counts would test both the concentration of radioisotopes in the mantle and crust, as well as the possible presence of  $^{40}\text{K}$  in the core.

### C. Uncertainties

We want to investigate the impact of uncertainties of the reference model on the geoneutrino distribution. The uncertainties for crust and mantle are independent of each other. The crust itself can vary by about a factor of 2 in radioisotope abundances and thus in geoneutrino intensity [10]. The net effect of these variations thus depends on how the crust and mantle uncertainties combine.



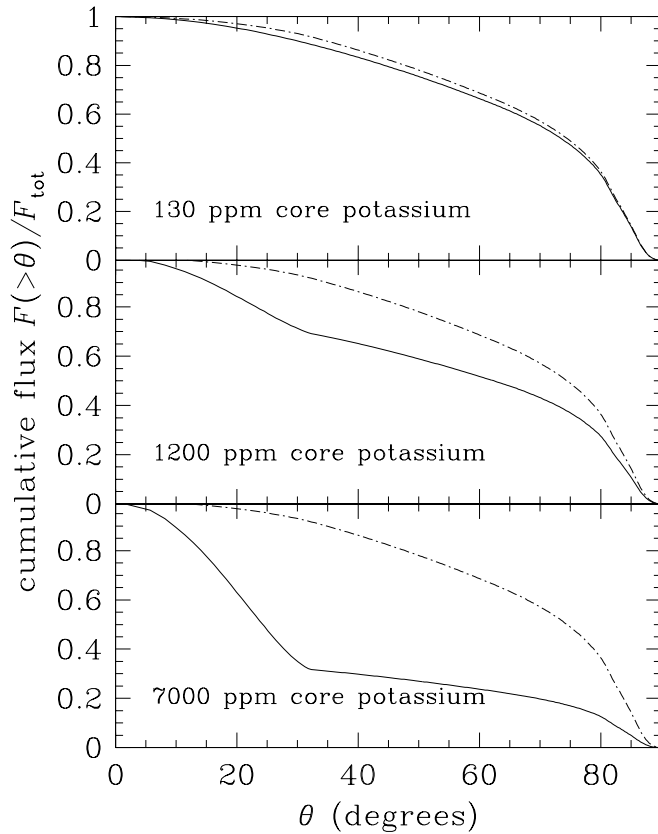


FIG. 7: The plots are similar to Fig. 6, except that they show the cumulative flux, normalized as in Fig. 5. The dashed line is the flux of the reference model.

Figure 8 shows some of the possible uncertainties. In the plot showing the minimum amount of radioactive elements in the crust-mantle system it can be perceived, that the reference model is on the low side of the possible abundances in comparison to the maximum abundances, where the intensity grows by a factor of two. The absence of a double peak in the intensity is due to the fact, that in [10] only a uncertainty for the whole crust is given, which does not take into account the distinction between lower, middle and upper crust. The overall shape of the maximum and minimum abundance plots stays overall very similar to the reference model, although there is a deviation from the general form at angles  $\theta \gtrsim 30^\circ$ . Thus we see that in all cases there appears a large peripheral flux, which remains a robust and highly testable prediction of this model.

For a more detailed analysis it will be necessary to construct a model of the outermost layer of the Earth, as we assumed for a change in altitude an increase in the number of neutrinos coming

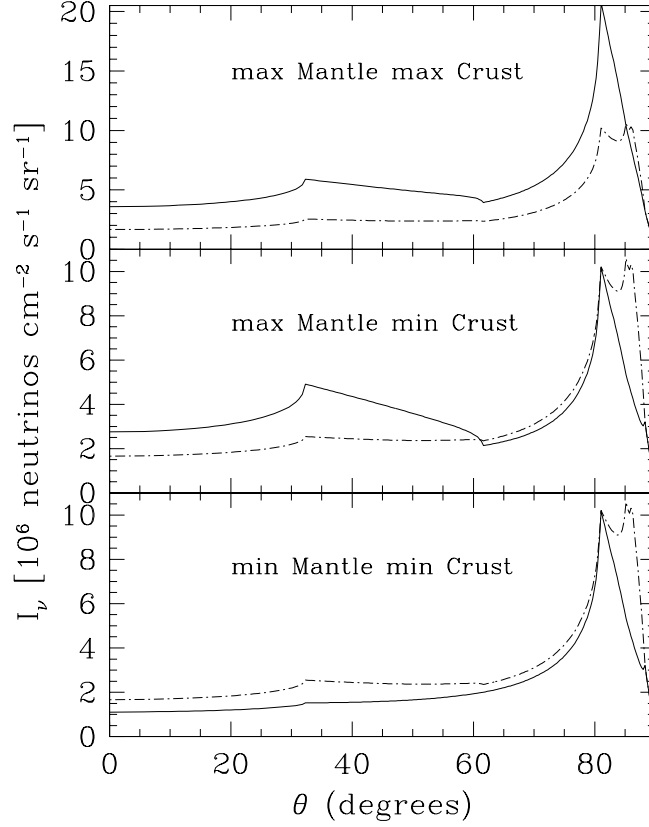


FIG. 8: The upper plot shows the intensity with a maximal amount of radioactive elements in crust and mantle. In the lower panel the intensity for a minimal abundance in crust and mantle is plotted. As the uncertainties in the abundances of mantle and crust are independent of each other [10], the plot in the middle shows a hybrid scenario with a maximal abundance in the mantle, whereas the crust abundance is minimized. The dashed-dotted line in all three plots is the reference model intensity is added as dashed dotted line in all three plots as comparison. It can be seen that the reference model is rather at the low side of the possible range of abundances. That the crust is only represented by a single peak is an artifact which arises because the uncertainties given in [10] do not distinguish between the different layers of the crust; this changes the intensity in the outer crust significantly.

from the sediments. But in any case the crudeness of our estimate only infects the results for the outer periphery, and the central angles remain reliable, as we now see.

#### D. Crust Anisotropies and Observing Strategies

We have assumed spherical symmetry throughout, and thus our calculations cannot directly address the effect of anisotropies in the radioisotope distributions. Yet these anisotropies, which reside in the crust, can have a very significant impact [10], since the crust is the largest radioisotope reservoir. For example, Mantovani et al. [10] predict fluxes which differ by more than a factor of 2 between locations above minimum and maximum crust depths. This would lead to changes in the overall geoneutrino intensity, and possibly to observable azimuthal asymmetry.

We note that emission from the crust will affect the intensity only at the largest nadir angles. Thus we expect our spherical calculation to be reliable at small to median angles. Furthermore, one can get a rough understanding of the effect of different crust depths by adopting spherical models in which the crust layers have the properties appropriate for the experimental location.

To consider an extreme example, consider a hypothetical model where we assume that the neutrino detector is on a ship. That means that the crust has the abundances of the oceanic crust and the top layer is three kilometers of ocean water. Of course in this case there is no sufficient shielding from cosmic rays and atmospheric radiation, which will make the detection of low energy neutrinos hard if not impossible. But never the less the effects are interesting, as the contribution coming from large angles is reduced by a factor of three, which should make it easier to detect the effects coming from the core and mantle. We have presently no model for an anisotropic Earth, but we expect, that for the real Earth in the described case the intensity for lower angles ( $\theta \lesssim 60^\circ$ ) will be very similar to the reference model (in case of its correctness), only the contribution from the angles  $\gtrsim 30^\circ$  will be noticeably reduced.

#### V. DISCUSSION

Geoneutrinos offer invaluable and unique information about the energetics and structure of the Earth [5, 8]. The longstanding dream of measuring this neutrino population has now begun to be realized with the first detection of a geophysical signal by the KamLAND experiment [6]. This achievement is already a triumph, as the geophysical component is (by design!) dominated by the signal from reactor neutrinos. Nevertheless, we believe it is now worthwhile to look forward to the even more challenging results of determining the angular distribution of geoneutrinos, which offers a wealth of new information.

In this paper we thus have calculated the angular distribution of geoneutrinos which arise

in  $\beta$ -decays of potassium, thorium, and uranium. We have developed the general formalism for the neutrino intensity in a spherically symmetric Earth. We find that the geoneutrino angular distribution, once known, can be inverted to fully recover the terrestrial radioisotope distribution. Thus the geoneutrino “sky” can provide a tomography of the Earth’s structure, and yields the full radial dependence of the radiogenic heat production.

Turning to model-building, we explore the idealized case of an arbitrary shell of uniform density. This can be generalized to give an Earth model which is a series of uniform shells. We then adopt the radioisotope profile of the Mantovani et al. reference model [10] and calculate the resulting angular distribution (Fig. 4). Because the reference model places all radioisotopes in the mantle and crust, the resulting geoneutrino intensity is highly “peripheral,” with 2/3 of the flux coming from nadir angles  $\theta \gtrsim 60^\circ$ . Thus, even a crude measurement of the angular distribution (say, in three  $30^\circ$  bins) would strongly test this prediction.

We have also investigated the effect of physically plausible variations to the reference model. Mantovani et al. [10] identify uncertainties in their radioisotope distributions which have the effect of multiplicatively raising or lowering the neutrino intensity, without a significant change to the angular shape. However, both the shape and normalization of the intensity can change strongly if the Earth’s core contains a significant amount of potassium, contrary to the assumptions of the reference model. If core potassium abundances are near the current upper limits [13], the resulting geoneutrino signal can dominate the total flux. Measurement of the angular distribution will probe the radioisotope abundances in the core. In particular, measurement of the intensity inside a nadir angle  $\theta \lesssim 30^\circ$  can discriminate among possibilities recently suggested in the literature.

Moreover, the central and peripheral intensities are related, since the peripheral neutrinos come from outer shells which also contribute to the central signal. Thus a measurement of the peripheral flux can be used to place a lower limit to the central flux. A difference between this lower limit and the observed central flux then amounts to a detection of some radioisotopes in the core.

A determination of the geoneutrino angular distribution will also solidify the connection between the geothermal heat flux and the geoneutrino flux. As noted by [8], the *radial* component of the neutrino flux is directly related, by Gauss’ law, to the geothermal heat production (eq. 24). But neutrino emission is locally isotropic and hence contains non-radial components; thus the angle-integrated geoneutrino flux in turn includes the non-radial components, and thus can only be related to the heat flux given a model of the radioisotope density profile. However, a measurement of the geoneutrino angular distribution can be inverted to recover the terrestrial radioisotope density distribution. This will allow for a full calculation not only of the global radiogenic heat production,

but also of its radial dependence. Thus one can test in detail models of heat production and transport.

In this way, the neutrino intensity can be used to measure the radioactive contribution to the geothermal heat flux. This can then be compared to geophysical measurements [1] of the total heat flux. A comparison of these results will yield a new and robust measurement of the Urey ratio (eq. 1) [2]. This in turn will shed light on the thermal history of the Earth, and quantify the importance of any non-radioactive heating, presumably due to residual “primordial” processes during the formation of the Earth.

Also, we note that the reference model we have adopted normalizes to the observed terrestrial heat flux and a Urey ratio of 0.5. Thus, if this Urey ratio is correct, but the heat flux contains a significant component from the core, this will reduce the contribution from the outer layers, which will act to redistribute the peripheral intensity to the interior.

These particular results illustrate a larger more general conclusion, that geoneutrinos open a new window to the Earth’s interior. Measurement of the angular distribution of geoneutrinos will allow us to infer the radioisotope distribution of the Earth. This in turn offers a new probe of the Earth’s structure—for example, allowing a test of how sharp the radioisotope boundaries are in going from crust to mantle to core. If the boundaries are sharp, then the angular distribution will offer unprecedented new measures of the positions of these boundaries and thus will be a general probe of the interior structure of the Earth.

What are the practical prospects of measuring the geoneutrino angular distribution? A complete discussion is beyond the scope of this paper, but it seems to us that there is some reason for hope. Antineutrinos are usually detected via inverse  $\beta$ -decay of protons,  $\bar{\nu}_e + p \rightarrow e^+ + n$ , and the subsequent observation of the rapid  $e^+$  annihilation signal as well as the delayed  $n$  capture onto an ambient nucleus. Part of the momentum of the neutrino is transferred to the neutron, which thus contains directional information. This directionality is however lost if the neutron scatters before it is captured. Thus, directional sensitivity is best for liquid scintillators which use materials (such as gadolinium) which a large neutron capture cross section. At present, no such measurement appears possible: KamLAND is a liquid scintillator experiment, but the scintillator is an organic material which does not have a large neutron capture cross section. However, the reactor neutrino experiment CHOOZ did use gadolinium scintillator, and was able to reconstruct the source direction to within about  $\sim 20^\circ$  [25], which as we have emphasized would already be geophysically interesting. While CHOOZ is no longer operating, and was too small to detect the geoneutrino intensity, it nevertheless demonstrated that antineutrinos with an energy spectrum

similar to that of geoneutrinos can be already detected with modest angular sensitivity.

We thus strongly hope that experimental effort be undertaken to measure the angular distribution of geoneutrinos. In particular, we suggest the construction of a scintillator antineutrino experiment using a medium with a large neutron capture cross section, such as gadolinium. Indeed, there has been recent interest in somewhat similar experiments to measure the higher-energy signal from the cosmic supernova antineutrino background [26, 27]. While the geoneutrino flux is significantly higher than the supernova background, geoneutrino detection will be all the more challenging given that typical geoneutrino energies are relatively low,  $\sim 0.5 - 1.5$  MeV [5, 10]. And of course, a good geoneutrino experiment clearly will need to be as far as possible from reactors (and possibly submarines!). This is particularly important if the radioisotope distribution really is concentrated in the outer Earth, as this will lead to a peripheral flux which can be confused with (but possibly calibrated by) the contribution from nearby detectors.

We note as well that we have so far considered the total, energy-integrated, intensity. However, neutrino energy information is also available, and indeed geoneutrino spectra have been presented [10]. Since the emitted energy spectra take the well-understood  $\beta$ -decay form, with sufficient energy resolution it is possible to separate the U, Th, and K components. If this can be done in conjunction with even the crudest angular resolution, it would be possible to actually distinguish beyond all doubt between neutrinos coming from U, Th and K and to obtain a particularly complete picture of the radioactive Earth.

Thus we believe the quest to measure an image of the “geoneutrino sky” is a worthy if challenging goal. As we have shown, even the first, crudest attempts at neutrino imaging will yield important results, and will thus impel further improvements. It is our hope that this paper encourages these efforts.

### **Acknowledgments**

We are grateful to Stuart Freedman for very helpful discussion regarding experimental issues and prospects regarding antineutrino directional sensitivity. We thank Charles Gammie for encouragement and for alerting us to the Abel transform, and V. Rama Murthy for enlightening discussions regarding core potassium. The work of BDF is supported by the National Science Foundation grant AST-0092939.

## APPENDIX A: TERRESTRIAL TOMOGRAPHY: INVERTING THE ANGULAR DISTRIBUTION

We may write the intensity distribution (eq. 6) in dimensionless units as

$$I(\sigma) = 2R_{\oplus} \int_{\sigma}^1 dx \frac{x q(x)}{\sqrt{x^2 - \sigma^2}} \equiv \int_0^{\sigma} dx K(\sigma, x) q(x) \quad (\text{A1})$$

where  $\sigma = \sin \theta \in [0, 1]$  and  $x = r/R_{\oplus} \in [0, 1]$ . Thus both  $I$  and  $q$  are defined on the interval  $[0, 1]$ . Furthermore, for an experiment on the surface of the Earth, we expect that  $I(1) = 0 = q(1)$  because the Earth's density goes to zero at the surface (by definition!). However, a real experiment located slightly under the surface of the Earth might have a nonzero horizontal flux  $I(1)$ .

Clearly,  $I(\sigma)$  is an integral transformation, with  $K(\sigma, x) = x/\sqrt{x^2 - \sigma^2}$  the kernel. Specifically, eq. (A1) is a version of the Abel transform [16]. In fact, the usual Abel transform is applied to a function defined over an infinite domain, but fortunately one can show that the key results carry over to our case of a finite domain.

The inverse Abel transform appropriate for our case is

$$q(x) = -\frac{1}{\pi R_{\oplus}} \int_x^1 d\sigma \frac{I'(\sigma)}{\sqrt{\sigma^2 - x^2}} + \frac{I(1)}{\pi R_{\oplus} \sqrt{1 - x^2}} \quad (\text{A2})$$

$$= -\int_0^{\sqrt{1-x^2}} d\mu \frac{I'(\mu)}{\sqrt{1-x^2-\mu^2}} + \frac{I(\mu=0)}{\pi R_{\oplus} \sqrt{1-x^2}} \quad (\text{A3})$$

$$(\text{A4})$$

where  $\mu = \cos \theta$ , and  $I'(y) = dI(y)/dy$  is the usual derivative.

Equation (A2) thus demonstrates by construction that, given a complete knowledge of the intensity distribution, one can fully recover the radioisotope source distribution. Thus, measurement of the geoneutrino angular distribution truly does carry the promise of tomographic imaging of the Earth's interior. In addition, with  $q(x)$  in hand, one can completely determine the radiogenic heat production of the Earth, both globally and as a function of depth.

Furthermore, eq. (A2) has the properties one would expect on physical grounds. The density at  $r = R_{\oplus}x$  depends only on the intensity derivative for the region  $\sin \theta \geq x$ , i.e., angles along or exterior to the tangent angle. Thus, inferring the outer density structure requires only knowledge of the peripheral intensity. On the other hand, to recover the inner density structure requires both peripheral and central intensities. This is indeed sensible if one thinks of the angular distribution roughly as a linear combination of intensities along the line of sight: outer angles have only a few "terms" in the sum, while inner angles contain all "terms."

One consequence of this result is that the peripheral intensity constrains the central intensity, by setting a lower limit on it. If we consider  $I(\sigma)$  only for  $\sigma > \sigma_0$ , we can infer a lower limit  $q_{\min}$  to the density distribution at  $x < \sigma_0$ , namely

$$q(x) > q_{\min}(x) = -\frac{1}{\pi R_{\oplus}} \int_{\sigma_0}^1 d\sigma \frac{I'(\sigma)}{\sqrt{\sigma^2 - x^2}} \quad (\text{A5})$$

This example illustrates that even with an incomplete or low-resolution determination of the intensity pattern, one can draw powerful physical conclusions.

- 
- [1] C. Stein, in *Global Earth Physics: A Handbook of Physical Constants*, AGU Reference Shelf 1, ed. T.J. Ahrens (American Geophysical Union, Washington, 1995), 144.
  - [2] D. McKenzie, F. Richter, *J. geophys. Res.* **86**, 11667 (1981)
  - [3] F. Albarede, R. van der Hilst, *Phil. Trans. R. Soc. Lond. A* **360**, 2569 (2002)
  - [4] G. Eder, *Nucl. Phys.* **78**, 657 (1966)
  - [5] L. M. Krauss, S. L. Glashow and D. N. Schramm, *Nature* **310**, 191 (1984).
  - [6] K. Eguchi *et al.* [KamLAND Collaboration], *Phys. Rev. Lett.* **90**, 021802 (2003) [arXiv:hep-ex/0212021].
  - [7] C. G. Rothschild, M. C. Chen and F. P. Calaprice, *Geophys. Res. Lett.* **25**, 1083 (1998) [arXiv:nucl-ex/9710001].
  - [8] G. Fiorentini, F. Mantovani and B. Ricci, *Phys. Lett. B* **557**, 139 (2003) [arXiv:nucl-ex/0212008].
  - [9] G. Fiorentini, T. Lasserre, M. Lissia, B. Ricci and S. Schonert, *Phys. Lett. B* **558**, 15 (2003) [arXiv:hep-ph/0301042].
  - [10] F. Mantovani, L. Carmignani, G. Fiorentini and M. Lissia, *Phys. Rev. D* **69**, 013001 (2004) [arXiv:hep-ph/0309013].
  - [11] H. Nunokawa, W. J. C. Teves and R. Zukanovich Funchal, *JHEP* **0311**, 020 (2003) [arXiv:hep-ph/0308175].
  - [12] V. Rama Murthy, W. van Westrenen, Y. Fei, *Nature* **423** (2003)
  - [13] K.K.M. Lee, R. Jeanloz, *Geophys.Res.Lett* **30** (2003)
  - [14] C.K. Gessmann, B.J. Wood, *Earth Planet. Sci. Lett.* **200**, p.63-78 (2002)
  - [15] S. Chandrasekhar, *Radiative Transfer* (Oxford University Press, Oxford, 1950), Chap. 1.
  - [16] R. N. Bracewell, *The Fourier transform and its applications*, (McGraw-Hill, New York, 1986)
  - [17] J. Binney and S. Tremaine, "Galactic Dynamics," Princeton: Princeton U. Press (1987)
  - [18] F.A. Dahlen, *Geophys. J. Int.* **157**, 315 (2004).
  - [19] V. Barger, K. Whisnant, S. Pakvasa, R. Phillips, in *Solar Neutrinos-The First 30 years*, ed. J.N. Bahcall et al. (Addison-Wesley, Reading, 1994), 300.
  - [20] G. L. Fogli, E. Lisi, A. Marrone, D. Montanino, A. Palazzo and A. M. Rotunno, *Phys. Rev. D* **67**, 073002 (2003) [arXiv:hep-ph/0212127].



- [21] A.M. Dziewonski and D.L. Anderson, Phys. Earth Plan. Int. **25**, 297 (1981).  
[http://solid\\_Earth.ou.edu/prem.html](http://solid_Earth.ou.edu/prem.html)
- [22] W. McDonough  
<http://mahi.ucsd.edu/cathy/SEDI2002/ABST/SEDI1-2.html>
- [23] G.J. Wasserburg, Gordon J.F. MacDonald, F. Hoyle, William A. Fowler, Science **143**, pp.465 (1964)
- [24] W.R. Van Schmus, Global Earth Physics: A Handbook of Physical Constants, AGU Reference Shelf 1, ed. T.J. Ahrens (American Geophysical Union, Washington, 1995), 283.
- [25] M. Apollonio *et al.* [CHOOZ Collaboration], Phys. Rev. D **61**, 012001 (2000) [arXiv:hep-ex/9906011].
- [26] J. F. Beacom and M. R. Vagins, arXiv:hep-ph/0309300.
- [27] L. Oberauer, Mod. Phys. Lett. A **19**, 337 (2004) [arXiv:hep-ph/0402162].